

constant within each species. All fish continued to swim and feed visually with no evidence of a lack of motivation.

Received 29 February; accepted 1 August 1997.

1. Arnold, G. P. Rheotrophism in fishes. *Biol. Rev.* **49**, 515–576 (1974).
2. Münz, H. in *The Mechanosensory Lateral Line Neurobiology and Evolution* (eds Coombs, S., Gorner, P. & Münz, H.) 285–298 (Springer, New York, 1989).
3. Dijkstra, S. in *The Mechanosensory Lateral Line Neurobiology and Evolution* (eds Coombs, S., Gorner, P. & Münz, H.) 7–14 (Springer, New York, 1989).
4. Montgomery, J. C., Coombs, S. & Halstead, M. Biology of the mechanosensory lateral line in fishes. *Rev. Fish Biol. Fish.* **5**, 399–416 (1995).
5. Coombs, S. & Montgomery, J. C. Function and evolution of superficial neuromasts in an antarctic nototheniid fish. *Brain Behav. Evol.* **44**, 287–298 (1994).
6. Montgomery, J. C. & Milton, R. C. Use of the lateral line for feeding in the Torrent fish (*Cheimarrichthys fosteri*). *N. Z. J. Zool.* **20**, 121–125 (1993).
7. Montgomery, J. C. & Macdonald, J. A. Sensory tuning of lateral line receptors in Antarctic fish to the movements of planktonic prey. *Science* **235**, 195–196 (1987).
8. Abdel-Latif, H., Hassan, E. S. & von Campenhausen, C. Sensory performance of blind Mexican cave fish after destruction of the canal neuromasts. *Naturwissenschaften* **77**, 237–239 (1990).
9. Karlsen, H. E. & Sand, O. Selective and reversible blocking of the lateral line in freshwater fish. *J. Exp. Biol.* **133**, 249–262 (1987).
10. Kroese, A. B. A. & van den Bercken, J. Effects of ototoxic antibiotics on sensory hair cell functioning. *Hearing Res.* **6**, 183–197 (1982).
11. Song, J., Yan, H. Y. & Popper, A. N. Damage and recovery of hair cells in fish canal (but not superficial) neuromasts after gentamicin exposure. *Hear. Res.* **91**, 63–71 (1995).
12. Montgomery, J. C. & Pankhurst, N. W. in *Deep-sea Fish* (eds Randall, D. J. & Farrell, A. P.) 325–349 (Academic, San Diego, 1997).
13. Able, K. P. & Able, M. A. Interactions in the flexible orientation system of a migratory bird. *Nature* **375**, 230–232 (1995).
14. Baxter, J. H. S. & Fuiman, L. A. in *The Mechanosensory Lateral Line Neurobiology and Evolution* (eds Coombs, S., Gorner, P. & Münz, H.) 481–499 (Springer, New York, 1989).
15. Andriashev, A. P. & Jakubowski, M. Morphological grounds for generic separation of the Antarctic broadhead-fishes (*Trematomus borchgrevincki*) Boulenger and *T. brachysoma* Pappenheim) and a new status of the genus *Pagothenia* Nichols et Lamonte (Nototheniidae). *Zool. Zh.* **50**, 1041–1055 (1971).
16. Schemmel, C. Vergleichende Untersuchungen an den Hautsinnesorganen ober- und unterirdisch lebender *Astyranax*-Formen ein Beitrag zur Evolution der Cavernicolen. *Z. Morphol. Tiere* **61**, 255–316 (1967).

Acknowledgements. We thank the Marsden Fund for support, Kelly Tarlton's Underwater World for an Antarctic scholarship and Carol Diebel for at times acting in loco mentis.

Correspondence and requests for materials should be addressed to J.C.M. (e-mail: j.montgomery@auckland.ac.nz).

Mutation of an axonemal dynein affects left-right asymmetry in *inversus viscerum* mice

Dorothy M. Supp*, David P. Witte†, S. Steven Potter* & Martina Brueckner‡

Divisions of *Development Biology and †Pathology, The Children's Hospital Research Foundation, Cincinnati, Ohio 45229, USA

‡Department of Pediatrics/Cardiology, Yale School of Medicine, New Haven, Connecticut 06520, USA

The development of characteristic visceral asymmetries along the left–right (LR) axis in an initially bilaterally symmetrical embryo is an essential feature of vertebrate patterning. The allelic mouse mutations *inversus viscerum* (*iv*)^{1,2} and *legless* (*lgl*)^{3,4} produce LR inversion, or situs inversus, in half of live-born homozygotes. This suggests that the *iv* gene product drives correct LR determination, and in its absence this process is randomized². These mutations provide tools for studying the development of LR-handed asymmetry and provide mouse models of human lateralization defects. At the molecular level, the normally LR asymmetric expression patterns of *nodal*⁵ and *lefty*⁶ are randomized in *iv/iv* embryos, suggesting that *iv* functions early in the genetic hierarchy of LR specification. Here we report the positional cloning of an axonemal dynein heavy-chain gene, *left/right-dynein* (*lrd*), that is mutated in both *lgl* and *iv*. *lrd* is expressed in the node of the embryo at embryonic day 7.5, consistent with its having a role in LR development⁷. Our findings indicate that dynein, a microtubule-based motor, is involved in the determination of LR-handed asymmetry and provide insight into the early molecular mechanisms of this process.

In humans, random development of left–right asymmetry is a feature of Kartagener's syndrome, which is manifested by situs inversus, immotile cilia and the absence of ciliary dynein arms; this suggests that dynein function has a role in LR development^{8,9}. Dyneins are a family of minus-end-directed microtubule-based motors which are traditionally classified as either cytoplasmic or axonemal. Cytoplasmic dyneins have been implicated in vesicular transport, nuclear migration, and spindle orientation^{10,11}, whereas axonemal dyneins produce the motive forces that cause the sliding of adjacent microtubules in the axoneme^{10,11} and thus produce ciliary and flagellar movement. Dyneins function as large multi-subunit complexes containing up to three heavy chains, which include the force-producing motor domain, in addition to several intermediate and light chains. So far, 15 distinct dynein heavy-chain genes have been identified in vertebrates^{12–14}. Two of these (*Dnchc1* and *Dnahc13*) were mapped to the distal region of mouse chromosome 12, close to the previously identified map location of the *iv* and *lgl* mutations^{4,15}.

We isolated and analysed overlapping YAC (yeast artificial chromosome) clones spanning the *lgl* transgene insertion site in this region of chromosome 12, which indicated that the *lgl* mutation includes a deletion of at least 600 kilobases (kb) (Fig. 1a). Our inability to isolate non-chimaeric YACs at one end of the contig or to identify the remaining mouse DNA–transgene junction suggests that this deletion may extend to the end of the chromosome. To determine whether a dynein gene is involved in the *iv* and *lgl* mutations, we screened the *lgl* YAC contig at low stringency with a DNA probe for the highly conserved first P-loop nucleotide-binding domain found in both cytoplasmic and axonemal dynein. This strategy identified a 2.1-kb genomic *Bgl*II fragment which cross-hybridizes to the dynein P-loop probe and is deleted in *lgl* DNA (see Supplementary information). Sequence analysis of this fragment revealed that it is distinct from *Dnchc1* and *Dnahc13* and includes two exons orthologous to a rat dynein-like gene, *DLP11* (ref. 12). We cloned over 7 kb of coding sequence from this gene, including all four central P-loops, and sequence analysis reveals 67% identity and 81% similarity to the sea-urchin axonemal dynein- β heavy-chain gene, compared with only 31% identity and 54% similarity to the rat cytoplasmic dynein heavy-chain gene (Fig. 1b). In

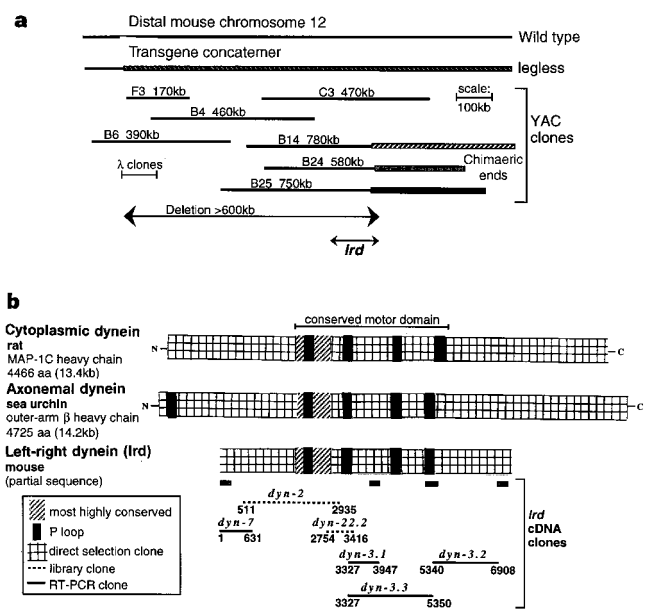


Figure 1 Identification of a dynein gene deleted in *lgl*. **a**, YAC contig spanning the mouse DNA/transgene junction in *lgl*. The location of the newly identified *lrd* gene (see text) is indicated. **b**, Homology of cloned *lrd* sequences with rat cytoplasmic and sea-urchin axonemal dynein heavy chains.

addition, the sequence immediately adjacent to the first P-loop (TETTKDL) defines this gene as an axonemal dynein isoform¹⁶. Recombination mapping using the same C57BL/6J X SJ/Col-*iv* outcross/backcross panel initially used to determine the map position of *iv* (ref. 17) demonstrated no recombination between this gene, which we designate *left/right-dynein* (*lrd*), and *iv* out of 39 informative meioses, including the one animal that exhibited a recombination event between the distal end of IgH-V and *iv*¹⁷ (data not shown).

Comparison of *lrd* sequences from wild type and *iv* demonstrates a striking missense mutation in *iv* mice. Analysis of 7 kb of sequence obtained from cloned reverse transcription polymerase chain reaction (RT-PCR) products from wild-type (ICR outbred mice) and *iv*/*iv* homozygous mice revealed six silent base changes that did not alter coding potential, and are therefore probably strain polymorphisms. However, one difference was found that changes a glutamic acid to a lysine at a position corresponding to residue 2,249 of the sea-urchin sequence (Fig. 2a). This amino-acid substitution, resulting in a change from negative to positive charge, is located between the second and third P-loop motifs. This region of the protein is part of the highly conserved central portion of the heavy chain that constitutes the motor domain¹⁰ (Fig. 1b). The G → A base change in *iv* was confirmed by sequencing RT-PCR products from multiple RNA preparations and by sequencing the relevant exon from genomic DNAs of multiple *iv* and wild-type mice. The *iv* mutation arose in an outbred stock of mice that was subsequently crossed into the strains DBA, C3H and BALB/c; hence no parental strain is available for comparison. Thus, to establish that the mutation did not represent a strain polymorphism, we sequenced the genomic DNA encompassing this region of the *lrd* gene from eight different strains of laboratory mice (C57BL/6J, C3H, BALB/c, A/J, AKR/J, DBA, 129/J and SJL/J), the wild-derived strains TIRANO/Ei (*Mus domesticus*), SPRET/Ei (*Mus spretus*), and PANCEVO/Ei (*Mus hortulanis*), as well as rat (*Rattus norvegicus*). All contain the wild-type glutamic acid at this position. As shown in Fig. 2b, this region of the protein is highly conserved across widely divergent species and among both axonemal and cytoplasmic

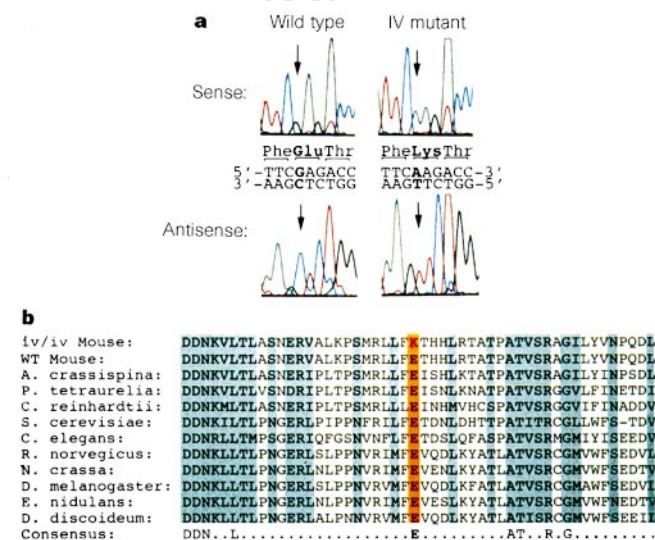


Figure 2 *iv* has a missense mutation in a highly conserved amino acid of *Lrd*. **a**, Raw sequence data. **b**, The E → K substitution is unique to *iv* and is in a very highly conserved amino-acid residue (orange). Amino acids that are identical or show only conservative changes across species are shaded. The consensus (bottom) shows residues that are identical among all known axonemal and cytoplasmic dynein sequences, including those not shown here. Amino-acid sequences in this region of *Lrd* were identical for all wild-type mouse strains analysed (12 in total). The rat orthologue also contains a glutamic acid at this position (data not shown).

dynein heavy chains. The glutamic acid residue at this position is absolutely conserved among all known dynein heavy-chain sequences, which suggests that it is critical to the function of the protein. We conclude that this glutamic acid-to-lysine substitution is unique to *iv* mutants and therefore provides a molecular basis for the randomization of LR development seen in these mice.

The *lgl* phenotype, with hindlimb, brain and craniofacial malformations, as well as situs inversus³, is more severe than the *iv* phenotype. This could be the result of a more severe *lrd* mutation in *lgl*—a deletion versus the missense mutation found in *iv*—and/or the result of additional genes mutated in *lgl* mice.

Expression of *lrd* messenger RNA was examined by northern blot hybridization, RT-PCR and *in situ* hybridization. Northern blot hybridization demonstrates a low abundance *lrd* transcript of ~15 kb in adult brain (see Supplementary information). Expression was detected at a lower level in adult testes (data not shown). The transcript size appears similar in *iv* and wild-type RNA. RT-PCR showed that *lrd* mRNA is expressed as early as the blastocyst stage (embryonic day (E) 3.5) and is also expressed in embryonic stem (ES) cells, which are derived from the blastocyst inner cell mass (Fig. 3). Expression is also seen at E8, E9 and E16.5 (Fig. 3). No transcripts were detected in mouse embryo fibroblasts (MEFs; Fig. 3). *In situ* hybridization showed that *lrd* mRNA embryonic expression is highly restricted; at E7.5, before the time of asymmetric expression of *nodal* and *lefty*, *lrd* mRNA is detected only in the ventral cells of the node (Fig. 4a–c). We detected no expression in the heart at any stage. These results show that the onset of *lrd* mRNA expression precedes that of *nodal* and *lefty*, two of the earliest molecular markers of LR asymmetry, which are misexpressed in *iv* mutant embryos.^{5,6} Also, the presence of *lrd* transcripts in the node implicates this mammalian equivalent of Spemann's organizer in the establishment of the LR axis. In the newborn and adult, expression of *lrd* mRNA was found in several types of ciliated epithelium, including the oviducts (Fig. 4d).

Expression of *lrd* mRNA in the embryo was observed primarily in non-ciliated cells, such as ES cells and blastocysts; it is unlikely that expression in the node is due to the presence of cilia, because cilia

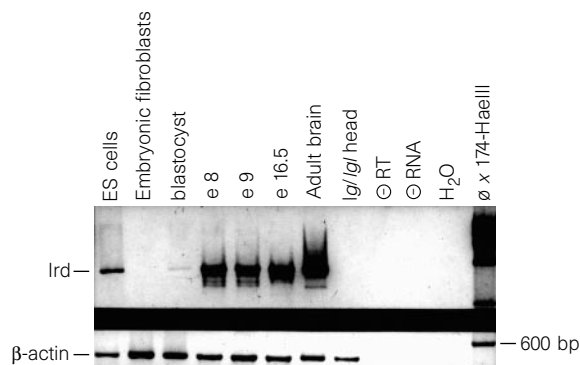
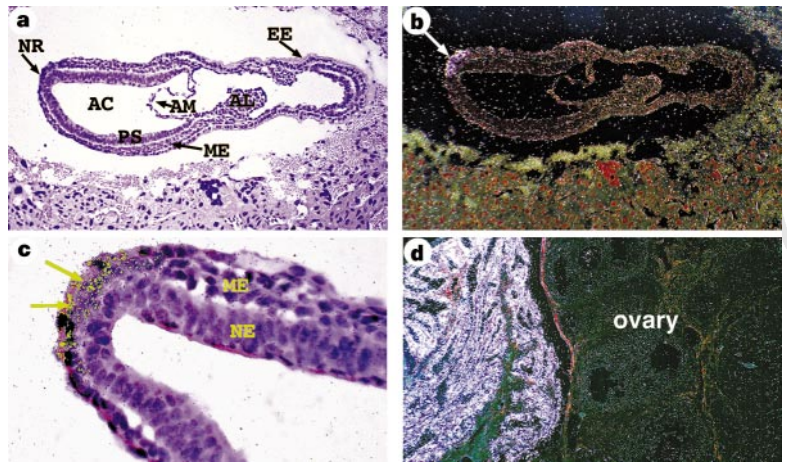


Figure 3 RT-PCR analysis of embryonic and adult expression. Primers used were specific for *lrd* (top) or control β -actin (bottom). Negative controls include: no reverse transcriptase (-RT), no tissue (medium control, -RNA), and no RNA (H₂O).

Figure 4 Expression of *lrd* localized by *in situ* hybridization. **a–d**, Hybridization to antisense *lrd* riboprobe; no signal was detected with a sense control probe. **a, c**, Bright-field image; **b, d**, dark-field images. **a, b**, Sagittal section of an E7.5 embryo demonstrating *lrd* expression in the node (arrow in **b**). **c**, Enlargement to show nodal localization of signal (arrows). **d**, *lrd* is expressed in the ciliated epithelium of the adult oviduct (left), but not in the ovary. NR, nodal region; AC, amniotic cavity; PS, primitive streak; AM, amnion; ME, mesoderm; AL, allantois; EE, extraembryonic ectoderm; NE, neural ectoderm. Computer-enhanced colour (yellow) was used to highlight the hybridization signal in **c**.



found in the node are immotile monocilia lacking dynein arms¹⁸. *lrd* mRNA expression was detected in many ciliated cells in the newborn and adult as well (Fig. 4d, and data not shown). As the sequence of *lrd* is more similar to axonemal than cytoplasmic dyneins, it is paradoxical that it is also found in cells lacking cilia; however, dyneins classified as axonemal have been found in non-ciliated cells¹⁹, suggesting that there is some blurring of the boundary between axonemal and cytoplasmic dyneins. We propose that *lrd* has dual functions: in the ciliated epithelium of adult structures it functions in ciliary beating, whereas embryonic expression indicates that mechanisms other than ciliary movement are involved in LR specification.

As a component of the dynein motor complex, *lrd* is an excellent candidate for involvement in LR determination, based on previous studies of dynein function and models of the development of handed asymmetry. As a microtubule-based motor, dynein might provide an initial LR bias to the embryo by asymmetric movement along a microtubule scaffolding which is oriented relative to the anterior–posterior and dorsal–ventral axes. Organized microtubule arrays are required for axis development in several model organisms^{20–22}. In *Xenopus*, for example, disruption of microtubule arrays in early embryos prevents cortical rotation and results in diminished dorsal–anterior development and randomized LR cardiac asymmetries²². Additionally, RNA encoding Vgl, a protein that can regulate *Xenopus* LR development²³, is asymmetrically localized to the vegetal cortex of the embryo through association with microtubules²⁴. These observations demonstrate the importance of microtubules in axis determination and the asymmetric localization of putative morphogens. Furthermore, the expression of *lrd* in the node is consistent with a role in LR specification, because several of the molecules implicated in LR development, such as *nodal*, *HNF-3 β* and *shh*, are also expressed there. A model of LR development²⁵ proposed the existence of handed molecules that are oriented with respect to the anterior–posterior and dorsal–ventral axes of the early embryo; these molecules would establish LR asymmetry by directional movements of morphogens. Based on our results showing that an axonemal dynein is mutated in *iv*, the handed molecules may be microtubules and dynein the molecular motor required to generate LR asymmetry. □

Methods

Mice. The *lgl* mutation has been described.³ *SI/Col-iv/iv* mice were obtained from Jackson Labs. For embryo isolation, noon on the day of finding a copulation plug (after overnight breeding) was considered as embryonic day 0.5. **YAC cloning.** F3, B4 and B6 YACs (Fig. 1a) were isolated as described²⁶. B14, B24 and B25 YACs were isolated from the Princeton YAC library screened with B4 YAC sequences (5′-GAAGAGCAGTCGGTGCTTTTACCAG-3′ and 5′CAGACAGTTGTGAGCCACTGGATATA-3′), and C3 was isolated from the Baylor mouse YAC library using the same primers. YAC end-specific fragments

were isolated as described²⁶, and interspecific backcross chromosome mapping (Jackson Labs Backcross DNA Panel Map Service) was used to show that B14, B24 and B25 are chimaeric; the right end of C3 contains repetitive sequences and was therefore not mapped. Probes from the left end of F3, the right end of B4, and all non-repetitive probes isolated from C3 are deleted in *lgl/lgl* DNA. ***lrd* gene isolation.** A 270-bp dynein P-loop probe was cloned from mouse brain cDNA with primers (5′-AACCTTGGATTCCAGGC-3′ and 5′-ATGGT-GATGAAGATAGCC-3′) based on conserved sequences flanking the first P-loop of the human and rat cytoplasmic dynein genes (GenBank accession numbers L23958 and L08505). This probe hybridized at reduced stringency (62°) to a 2.1-kb *Bgl*II fragment in C3, B14, B24 and B25 YAC DNAs. This cross-hybridizing fragment was cloned from a C3 YAC plasmid library and was used to screen adult mouse brain and testis cDNA libraries (Clontech) to isolate *dyn-2* and *dyn-22.2* cDNA clones.

The C3 YAC was used to clone additional cDNAs by direct cDNA selection as described²⁷, with the following modifications. cDNA prepared from wild-type adult brain mRNA using oligo(dT) and random primers and the Marathon cDNA-amplification kit (Clontech) was digested with *Alu*I, *Hae*III or *Rsa*I before linker addition and PCR amplification. cDNA was preblocked with 2 μ g Cot1 DNA (Gibco BRL) and 8 μ g *lgl/lgl* DNA to duplex repetitive and non-deleted sequences before hybridization. After two rounds of hybridization, selected cDNAs were subcloned into the pT7blue vector (Novagen).

RT-PCR using TaqStart Ab (Clontech) and Expand long-range PCR (Boehringer-Mannheim) was used to clone cDNAs connecting the library and direct selection cDNA sequences and to clone cDNAs from *iv/iv* mutant adult-brain RNA.

Chromosome mapping. Recombination mapping was done using the outcross/backcross panel previously described¹⁷. An 800-bp *Bst*XI restriction fragment probe from *dyn-2* cDNA detected a polymorphism between *SI/Col* and *C57BL/6J* DNA digested with *Pst*I, allowing the *C57BL/6J* portion of the backcross panel to be used.

Mutation analysis. The region of *lrd* encompassing the mutation in *iv* was amplified using the following primers: *dyn3.6* (5′-ATGATAA-CAAGGTGCTGACCC-3′), *dyn3.7* (5′-CAAAATGCCAGCTCTGGAGACC-3′), *dyn 3.6A* (5′-GCCAGCAATGAACGAGTGGCCCTCAAACCT-3′), and *dyn 3.7A* (5′-AGCTCTGGAACCGTGGCTGGTGTGGCTGT-3′). Primers *dyn3.6* and *dyn3.7* were used for RT-PCR to clone fragments from wild-type (Outbred ICR mice, Harlan) and *iv/iv* adult brain RNA. Three different RT-PCR clones per genotype, representing two different RNA samples, were analysed. For confirmation, these primers were used to isolate PCR products from genomic DNA of wild-type mouse strains DBA, 129/J, *C57BL/6J*, *C3H*, *SJL/J* and *Mus spretus*, as well as *iv/iv* (*SI/Col*), for direct sequencing with primers *dyn3.7* and *dyn3.8* (genomic-specific: 5′-TGAGTCTACCTGTGGCT-GTCC-3′). Additionally, primers *dyn3.6A* and *dyn3.7A* were used to clone PCR fragments from *SI/Col-iv/iv* and the wild-type strains (*C57BL/6J*, *C3H*, *BALB/c*, *A/J*, *AKR/J*, *SPRET/Ei* (*Mus spretus*), *PANCEVO/Ei* (*Mus hortulanus*), *TIRANO/Ei* (*Mus domesticus*) and rat (*Rattus norvegicus*). At least two independent clones per DNA were sequenced. DNAs were obtained from the Jackson Labs.

GenBank accession numbers for sequences shown in Fig. 2b: *Anthocardaris crassispina* (sea urchin) ciliary dynein- β heavy chain (D01021), *Paramecium tetraurelia* outer arm dynein- β heavy chain (U19464), *Chlamydomonas reinhardtii* dynein- β heavy chain (U02963), *Saccharomyces cerevisiae* cytoplasmic dynein heavy chain (Z21877), *Caenorhabditis elegans* dynein (Z75536), *Rattus norvegicus* cytoplasmic dynein heavy chain (L08505), *Neurospora crassa* cytoplasmic dynein heavy chain (P45443), *Drosophila melanogaster* cytoplasmic dynein heavy chain (P37276), *Emericella nidulans* cytoplasmic dynein (P45444), and *Dictyostelium discoideum* cytoplasmic dynein heavy chain (A44357).

RT-PCR. cDNA was prepared using SuperScript (Gibco BRL). PCR was done using Amplitaq Gold (Perkin-Elmer) and primers dyn3.3 (5'-AGAGCTT-CATCCTCAAAGTTGTC-3') and dyn3.5 (5'-CAACTGCCACATACG-GATTC-3') (94 °C for 30 s, 65 °C for 30 s, 72 °C for 30 s; 42 cycles).

In situ hybridization. Serial-section *in situ* hybridization was performed as described²⁸ with a cDNA probe from a non-conserved region of *lrd* (the most 3' 694 nucleotides of the sequence indicated in Fig. 1b); this probe does not cross-hybridize with other dynein genes by Southern blot analysis.

Received 15 July; accepted 16 September 1997.

- Hummel, K. P. & Chapman, D. B. Visceral inversion and associated anomalies in the mouse. *J. Hered.* **50**, 9–13 (1959).
- Layton, W. M. Random determination of a developmental process. *J. Hered.* **67**, 336–338 (1976).
- McNeish, J. D. *et al.* Phenotypic characterization of the transgenic mouse insertional mutation *Legless*. *J. Exp. Zool.* **253**, 151–162 (1990).
- Singh, G. *et al.* *legless* insertional mutation: morphological, molecular, and genetic characterization. *Genes Dev.* **5**, 2245–2255 (1991).
- Lowe, L. A. *et al.* Conserved left-right asymmetry of nodal expression and alterations in murine *situs inversus*. *Nature* **381**, 158–161 (1996).
- Meno, C. *et al.* Left-right asymmetric expression of the TGF β -family member *lefty* in mouse embryos. *Nature* **381**, 151–155 (1996).
- Lohr, J. L., Danos, M. C. & Yost, H. J. Left-right asymmetry of a *nodal*-related gene is regulated by dorsoanterior midline structures during *Xenopus* development. *Development* **124**, 1465–1472 (1997).
- Afzelius, B. A. A human syndrome caused by immotile cilia. *Science* **193**, 317–319 (1976).
- Afzelius, B. A. *Situs inversus* and ciliary abnormalities: What is the connection? *Int. J. Dev. Biol.* **39**, 839–844 (1995).
- Holzbaun, E. L. F. & Vallee, R. B. Dyneins: molecular structure and cellular function. *Annu. Rev. Cell Biol.* **10**, 339–372 (1994).
- Asai, D. J. Multi-dynein hypothesis. *Cell Motil. Cytoskel.* **32**, 129–132 (1995).
- Tanaka, Y., Zhang, Z. & Hirokawa, N. Identification and molecular evolution of new dynein-like protein sequences in rat brain. *J. Cell Sci.* **108**, 1883–1893 (1995).
- Vaughan, K. T. *et al.* Multiple mouse chromosomal loci for dynein-based motility. *Genomics* **36**, 29–38 (1996).
- Andrews, K. L., Nettesheim, P., Asai, D. J. & Ostrowski, L. E. Identification of seven rat axonemal dynein heavy chain genes: expression during ciliated cell differentiation. *Mol. Biol. Cell* **7**, 71–79 (1996).
- McGrath, J., Horwich, A. L. & Brueckner, M. Duplication/deficiency mapping of *situs inversus viscerum* (*iv*), a gene that determines left-right asymmetry in the mouse. *Genomics* **14**, 643–648 (1992).
- Asai, D. J. *et al.* The dynein genes of *Paramecium tetraurelia*: sequences adjacent to the catalytic P-loop identify cytoplasmic and axonemal heavy chain isoforms. *J. Cell Sci.* **107**, 839–847 (1994).
- Brueckner, M., D'Eustachio, P. & Horwich, A. L. Linkage mapping of a mouse gene, *iv*, that controls left-right asymmetry of the heart and viscera. *Proc. Natl Acad. Sci. USA* **86**, 5035–5038 (1989).
- Bellomo, D., Lander, A., Harragan, I. & Brown, N. A. Cell proliferation in mammalian gastrulation: the ventral node and notochord are relatively quiescent. *Dev. Dyn.* **205**, 471–485 (1996).
- Vaisberg, E. A., Grissom, P. M. & McIntosh, J. R. Mammalian cells express three distinct dynein heavy chains that are localized to different cytoplasmic organelles. *J. Cell Biol.* **133**, 831–841 (1996).
- Theurkauf, W. E. Microtubules and cytoplasm organization during *Drosophila* oogenesis. *Dev. Biol.* **165**, 352–360 (1994).
- Jesuthasan, S. & Strahle, U. Dynamic microtubules and specification of the zebrafish embryonic axis. *Curr. Biol.* **7**, 31–42 (1996).
- Danos, M. C. & Yost, H. J. Linkage of cardiac left-right asymmetry and dorsal-anterior development in *Xenopus*. *Development* **121**, 1467–1474 (1995).
- Hyatt, B. A., Lohr, J. L. & Yost, H. J. Initiation of vertebrate left-right axis formation by maternal *Vg1*. *Nature* **384**, 62–65 (1996).
- Elisha, Z., Havin, L., Ringel, I. & Yisraeli, J. K. *Vg1* RNA binding protein mediates the association of *Vg1* RNA with microtubules in *Xenopus* oocytes. *EMBO J.* **14**, 5109–5114 (1995).
- Brown, N. A., McCarthy, A. & Wolpert, L. Development of handed body asymmetry in mammals. *Ciba Found. Symp.* **162**, 182–201 (1991).
- Supp, D. M., Witte, D. P., Branford, W. W., Smith, E. P. & Potter, S. S. Sp4, a member of the Sp1-family of zinc finger transcription factors, is required for normal murine growth, viability, and male fertility. *Dev. Biol.* **176**, 284–299 (1996).
- Segre, J. A., Nemhauser, J. L., Taylor, B. A., Nadeau, J. H. & Lander, E. S. Positional cloning of the *nude* locus: genetic, physical, and transcription maps of the region and mutations in the mouse and rat. *Genomics* **28**, 549–559 (1995).
- Kern, M. J., Witte, D. P., Valerius, M. T., Aronow, B. J. & Potter, S. S. A novel murine homeobox gene isolated by a tissue specific PCR cloning strategy. *Nucleic Acids Res.* **20**, 5189–5195 (1992).

Supplementary information is available on Nature's World-Wide Web site (<http://www.nature.com>) or as paper copy from Mary Sheehan at the London editorial office of Nature.

Acknowledgements. We thank R. B. Vallee, M. A. Ghee and K. T. Vaughan for their comments and for providing a mouse cytoplasmic dynein cDNA probe; J. McGrath for assistance in embryo isolation; M. Lee for help with chromosome mapping; J. M. Corrales for help with cDNA cloning; K. Saalfeld, P. Groen and L. Artmeyer for *in situ* hybridization; A. Emley for photographic assistance; S. Bell for help with the expression studies; A. Horwich for comments and discussion; and the staff at the Keck Biotechnology Center at Yale University and at the University of Cincinnati DNA Core Facility for DNA sequencing. This work was supported by grants from the NIH (S.S.P. and D.M.S.), the American Heart Association, Ohio Division (D.P.W.), and The March of Dimes (M.B.).

Correspondence and requests for materials should be addressed to M.B. (e-mail: brueckner@biomed.med.yale.edu).

Wnt signalling required for expansion of neural crest and CNS progenitors

Makoto Ikeya*, Scott M. K. Lee†, Jane E. Johnson‡, Andrew P. McMahon† & Shinji Takada*

* Centre for Molecular and Developmental Biology, Faculty of Science, Kyoto University, Kitashirakawa, Sakyo-ku, Kyoto 606-01, Japan

† Department of Molecular and Cellular Biology, The Biolabs,

Harvard University, 16 Divinity Avenue, Cambridge, Massachusetts 02138, USA

‡ Cell Biology and Neuroscience, University of Texas Southwestern Medical Center, 5323 Harry Hines Boulevard, Dallas, Texas 75235, USA

Interactions between cells help to elaborate pattern within the vertebrate central nervous system (CNS)¹. The genes *Wnt-1* and *Wnt-3a*, which encode members of the Wnt family of cysteine-rich secreted signals, are coexpressed at the dorsal midline of the developing neural tube, coincident with dorsal patterning^{2,3}. Each signal is essential for embryonic development, *Wnt-1* for mid-brain patterning^{4,5} and *Wnt-3a* for formation of the paraxial mesoderm⁶, but the absence of a dorsal neural-tube phenotype in each mutant suggests that Wnt signalling may be redundant. Here we demonstrate that in the absence of both *Wnt-1* and *Wnt-3a* there is a marked deficiency in neural crest derivatives, which originate from the dorsal neural tube⁷, and a pronounced reduction in dorsolateral neural precursors within the neural tube itself. These phenotypes do not seem to result from a disruption in the mechanisms responsible for establishing normal dorsoventral polarity. Rather, our results are consistent with a model in which local Wnt signalling regulates the expansion of dorsal neural precursors. Given the widespread expression of different *Wnt* genes in discrete areas of the mammalian neural tube³, this may represent a general model for the action of Wnt signalling in the developing CNS.

The Wnt family of cysteine-rich signalling factors is composed of at least 16 members in the mouse. Four of these, *Wnt-1*, -3, -3a and -4, are expressed in largely overlapping regions within the dorsal CNS, predominantly at the dorsal midline from the forebrain to spinal cord³. Neural expression of the genes encoding *Wnt-1* and *Wnt-3a* occurs before that of other family members, coincident with neural-crest differentiation in the dorsal neural tube. Expression remains in the roofplate throughout the period of CNS neurogenesis^{2,3}. Null mutants in three of these *Wnt* genes have been described: *Wnt-1* regulates midbrain development^{4,5}, *Wnt-3a* regulates paraxial mesoderm formation⁶, and *Wnt-4* regulates kidney tubulogenesis⁸. None of these signals seems to be required for dorsal CNS development. However, cell transformation studies indicate that *Wnt-1* and *Wnt-3a* have similar activities⁹. Thus redundancy between Wnt signals may obscure a possible role for Wnt signalling in formation of the neural crest and in dorsoventral patterning of the vertebrate CNS.

To address this possibility we generated compound mutants lacking both *Wnt-1* and *Wnt-3a* signalling. Compound homozygotes were recovered at the expected mendelian frequency (51 compound homozygotes in 673 embryos, close to the expected frequency of 1/16) between 9.0 and 10.5 days post coitum (d.p.c.). However, owing to the termination of caudal axial development accompanying the loss of *Wnt-3a* activity, relatively few of these embryos survived to 18.5 d.p.c. (3 compound homozygotes in 151 embryos).

To assess the development of the dorsal neural tube in compound mutants we first examined structures derived from the neural crest. Neural crest cells are amongst the first differentiated cell types to be